Giant vortex in a fast rotating holographic superfluid

Jia-Hao Su,[1] Chuan-Yin Xia,[1] Wei-Can Yang,[1,2] and Hua-Bi Zeng[1,*]

[1]*Center for Gravitation and Cosmology, College of Physical Science and Technology, Yangzhou University, Yangzhou 225009, China*

[2]*Department of Physics, Osaka Metropolitan University, 3-3-138 Sugimoto, 558-8585 Osaka, Japan*

(Received 21 September 2022; accepted 7 December 2022; published 5 January 2023)

In a holographic superfluid disk, when the rotational velocity is large enough, we find that a giant vortex will form in the center of the system by merging several single charged vortices at some specific rotational velocity with a phase stratification phenomenon for the order parameter. The formation of a giant vortex can be explained, as there is not enough space for a standard vortex lattice. If we keep increasing the rotational velocity, the giant vortex will disappear and there will be an appearance of a superfluid ring. In the giant vortex region, the number of vortices measured from winding number and rotational velocity always satisfies the linear Feynman relation. However, when the superfluid ring starts to appear, the number of vortices in the disk will decrease although the rotational velocity is increasing, while most of the order parameter is suppressed.

DOI: 10.1103/PhysRevD.107.026006

I. INTRODUCTION

In quantum fluids such as superfluid, a lot of interesting and counterintuitive phenomena occur, for example, in a rotating vessel containing superfluid, when the rotation velocity is large enough, topological defects with integer winding number, also known as quantum vortices, will be generated from the nonrotating superfluid [1–5]. Based on the requirement of minimum free energy when the number of quantum vortices is enough, they will be arranged in the form of a lattice [6–9]. The vortices always have a winding number $N = 1$ since a giant vortex with $N > 1$ has a larger free energy than a single charged vortex system [10]. The superfluid vortex lattices were first observed in ^{3}He experiments [11–17]. Theoretical research on the properties of a vortex lattice relies mainly on numerical simulation by using the Gross-Pitaevskii (GP) equation, which is a mean field theory [18–23]. The GP equation describes the ground state of a quantum system of identical bosons by using the Hartree-Fock approximation and the pseudopotential interaction model, which can simulate various behaviors of the cold atomic Bose-Einstein condensation (BEC) well at zero temperature, including vortex lattice formation in rotational systems. For a single component superfluid, it is generously believed that a hexagonal vortex lattice will be formed; however, the situation seems to be changed by fast rotation, which has been studied for more than a decade [24–29]. In the simulation of the GP equation with a quadratic-plus-quartic potential [30], it is found that when the rotation velocity is large enough, the phase singularities will gather in the center and generate a "giant vortex" [31,32].

Although the GP equation is a powerful tool to study weakly interacting superfluid or BECs, it would be interesting to extend the study to the holographic superfluid, which is a strongly coupled system [33–35]. In addition, the finite temperature description of the GP equation comes from the artificially added dissipation coefficient, while in the holographic superfluid model the dissipation comes naturally from the black hole temperature [36–38]. At the end of the last century, Maldacena's great conjecture that the two perspectives in string theory are equivalent brought holographic duality theory into public view [33]. Based on this equivalence, a complete set of duality models was constructed—namely, the equivalence of a high-dimensional gravitational field and a low-dimensional quantum field living on its boundary [39,40]. In particular, when the large-N limit is considered, the gravitational field degenerates to classical gravity, while the quantum field has a property of strong interaction, yielded stunning success in the study of strongly coupled systems. This model can also be used to study condensed matter physics [41–43], such as holographic superconductivity [36–38]. There have been some previous studies of holographic superconductor and superfluid vortices [44–51], and the rotating superfluid dynamics evolution of vortices and Feynman relationship were studied at low rotation velocity [52–54]. However,

*hbzeng@yzu.edu.cn

research on the fast rotating holographic superfluid is still lacking.

In this paper, we use the finite temperature holographic superfluid model to study the vortex lattice properties of a fast rotating strongly coupled superfluid. We find that, at some special rotational velocity, the disk center will generate a stable giant vortex structure with a multiple winding number, which violates the general understanding that the energy of multiple winding number vortices is higher than the energy of the separated vortices [10]. As the rotation velocity continues to increase, we observe the phase of giant vortex stratification in the radial direction on the phase configuration chart. In an ultrafast rotating superfluid, the vortices are distributed in rings and the rings are isolated from each other. The outside part of it is a superfluid ring, and the inside part of it is a vortex ring.

The paper is organized as follows. In Sec. II we derive the fully expanded equation of motion of superfluid in the holographic model. In Sec. III we show the process of the time-dependent evolution at a specific rotational velocity where a giant vortex forms by the numerical solution of dynamic equations. And we obtain various configurations of vortices, including a giant vortex and a superfluid ring. In Sec. IV we discuss the relationship between the quantity of vortices N and the rotating velocity Ω. We summarize our results in Sec. V.

II. HOLOGRAPHIC MODEL AND EQUATIONS OF MOTION FOR TIME EVOLUTION

We construct the holographic superfluid model with a gauge field and a complex scalar field in the background of a planar Schwarzschild black hole in $(3+1)$-dimensional anti–de Sitter spacetime, which is dual to a $(2+1)$-dimensional conformal field theory on the boundary [36–38]. The action can be written as

$$S=\frac{1}{16\pi G_N}\int d^4x\sqrt{-g}\left[\mathcal{R}+6/L^2+\frac{1}{q^2}\mathcal{L}_{\text{matter}}\right], \quad (1)$$

where G_N is the Newton's constant, $\mathcal{R}$ is the Ricci scalar, and L is the radius of curvature of anti–de Sitter (AdS) spacetime. We work in the probe limit by taking the large-q limit, which means that the matter fields decouple from gravity. The matter field Lagrangian is

$$\mathcal{L}_{\text{matter}}=-\frac{1}{4}F_{\mu\nu}F^{\mu\nu}-|D_\mu\Psi|^2-m^2|\Psi|^2, \quad (2)$$

where $F_{\mu\nu}=\partial_\mu A_\nu-\partial_\nu A_\mu$ is a component of the U(1) gauge field and Ψ is a complex scalar field with mass m. D_μ is the covariant derivative written as

$$D_\mu\Psi=\partial_\mu\Psi-iq_sA_\mu\Psi. \quad (3)$$

We choose the Eddington-Finkelstein coordinate $\sqrt{-g}=L^4/z^4$, which has the form

$$\mathrm{d}s^2=L^2/z^2(-f(z)\mathrm{d}t^2-2\mathrm{d}t\mathrm{d}z+\mathrm{d}r^2+r^2\mathrm{d}\theta^2), \quad (4)$$

where $z=0$ represents the AdS boundary and $z=z_h$ is the horizon of the black hole. Without loss of generality, we can set $z_h=L=1$, then $f(z)=1-z^3$, and the Hawking temperature can be written as $T=3/4\pi$. The only characteristic parameter of the holographic superfluid is the dimensionless ratio μ/T, where $\mu=A_t(z=0)$ is the chemical potential on the boundary. Then the temperature on the boundary can be expressed as $T=(\mu_c/\mu)T_c$.

Then we can build a polar coordinate in a disk on the dual $(2+1)$-dimensional boundary to study the rotating superfluid. In this model, the black hole is nonrotating; thus, the superfluid is treated as static but the disk is rotating, which also has a relative rotation. With the action one can obtain the equation of motion for the scalar field

$$D^\mu D_\mu\Psi-m_s^2\Psi=0 \quad (5)$$

and the equation of motion for the vector field

$$\partial^\nu F_{\nu\mu}-iq_s(\Psi^*D_\mu\Psi-\Psi D_\mu\Psi^*)=0. \quad (6)$$

Here, according to the conservation principle, $J^\mu=i(\Psi^*D_\mu\Psi-\Psi D_\mu\Psi^*)$ is the bulk current. We take the ansatz of nonvanishing fields $\Psi(t,r,\theta,z)$, $A_t(t,r,\theta,z)$, $A_x(t,r,\theta,z)$, and $A_y(t,r,\theta,z)$, and the axial gauge $A_z=0$ is adopted as in Ref. [55]. With the ansatz, the fully expanded equations of motion can be written as

$$\begin{aligned}&-[\partial_z(f\partial_z\Psi)+i(\partial_zA_t)\Psi+2iA_t\partial_z\Psi]\\&+\left[-\partial_r^2\Psi+i(\partial_rA_r)\Psi+2iA_r\partial_r\Psi-\frac{1}{r}\partial_r\Psi\right]\\&+\frac{1}{r^2}[-\partial_\theta^2\Psi+i(\partial_\theta A_\theta)\Psi+2iA_\theta\partial_\theta\Psi]\\&+\left[A_r^2+\frac{iA_r}{r}+\frac{A_\theta^2}{r^2}+z\right]\Psi+2\partial_t\partial_z\Psi=0,\end{aligned} \quad (7)$$

$$\begin{aligned}&\partial_z^2A_t-\partial_z\partial_rA_r-\frac{1}{r}\partial_zA_r-\frac{1}{r^2}\partial_z\partial_\theta A_\theta\\&\quad-i(\Psi^*\partial_z\Psi-\Psi\partial_z\Psi^*)=0,\end{aligned} \quad (8)$$

$$\begin{aligned}&-\frac{1}{r}\partial_zA_r-\partial_t\partial_zA_t-\partial_t\partial_rA_r-\frac{1}{r^2}\partial_t\partial_\theta A_\theta+\frac{f}{r}\partial_zA_r\\&+f\partial_z\partial_rA_r+\frac{f}{r^2}\partial_z\partial_\theta A_\theta+\partial_r^2A_t+\frac{1}{r}\partial_rA_t+\frac{1}{r^2}\partial_\theta^2A_t\\&-i(\Psi^*\partial_t\Psi-\Psi\partial_t\Psi^*)-2A_t\Psi^*\Psi\\&+if(\Psi^*\partial_z\Psi-\Psi\partial_z\Psi^*)=0,\end{aligned} \quad (9)$$

$$2\partial_t\partial_z A_r - \partial_z\partial_r A_t - \partial_z(f\partial_z A_r) + \frac{1}{r^2}(\partial_r\partial_\theta A_\theta - \partial_\theta^2 A_r) + i(\Psi^*\partial_r\Psi - \Psi\partial_r\Psi^*) + 2A_r\Psi^*\Psi = 0, \tag{10}$$

$$2\partial_t\partial_z A_\theta - \partial_z(f\partial_z A_\theta) - \partial_z\partial_\theta A_t - \partial_r^2 A_\theta + \frac{1}{r}\partial_r A_\theta + \partial_r\partial_\theta A_r - \frac{1}{r}\partial_\theta A_r + i(\Psi^*\partial_\theta\Psi - \Psi\partial_\theta\Psi^*) + 2A_\theta\Psi^*\Psi = 0. \tag{11}$$

By taking $m_s^2 = -2$, the conformal dimension of the scalar field are $\Delta = \frac{3}{2} \pm \sqrt{\frac{9}{4} - m^2L^2} = \frac{3}{2} \pm \frac{1}{2}$, which means the expansion of the solution of the scalar field and gauge field near the AdS boundary has the form

$$\Psi = \phi z + \psi z^2 + \mathcal{O}(z^3), \tag{12}$$

$$A_\nu = a_\nu + b_\nu z + \mathcal{O}(z^2). \tag{13}$$

At the boundary $z = 0$, we turn off the source $\psi|_{z=0} = 0$. $a_t = \mu$ is the chemical potential and $b_t = \rho$ the charge. As we discussed above, μ is inversely proportional to temperature T when μ exceeds a critical value $\mu_c = 4.07$, the system spontaneously breaks the U(1) gauge symmetry and the expectation value of the scalar operator $\langle O\rangle = \phi|_{z=0}$ has a finite-valued solution. Since a_θ and a_r represent the superfluid velocity, we can add a rotation to the system without radial flow $a_r = 0$,

$$A_\theta|_{z=0} = a_\theta = \Omega r^2, \tag{14}$$

where Ω is the rigid rotation with angular velocity of the disk [49]. In this paper, we fix $T = 0.67T_c$, and the disk size radius $R = 5$.

For the numerical simulation, Chebyshev spectral method is used in the (z, r) direction. The Fourier spectral method is used in the θ direction. Time evolution is simulated by the fourth-order Runge-Kutta method. The initial configuration at $t = 0$ is chosen to be a homogeneous superfluid state without any rotation at the fixed temperature $T = 0.67T_c$.

III. THE STRUCTURES OF A GIANT VORTEX AND SUPERFLUID RING

If initially there is a nonrotating homogeneous superfluid state, then by setting the boundary condition to inject the angular momentum to the holographic superfluid will drive the system to evolve. The rotational velocity Ω ranges from 0.345 to 0.45, which is the slow rotation case, and the vortex lattice of the polygonal grid can be obtained in both the GP equation of mean field theory [18–23] and the holographic model [52,53]. In our simulation, after selecting the fast rotating velocity beyond this velocity range, we observed more special vortex structures. An example of the dynamic formation process of a giant vortex in a rapidly rotating superflow is shown in Fig. 1, and a movie is included in the Supplemental Material [56]. At $t = 0$, the superfluid disk was homogeneous. When we give an angular velocity to the disk, the vortices emerge on the boundary ($t = 500$), and they move inside and form the formation of a giant vortex appearing in a two-layer structure ($t = 2000$). There are four vortices arriving at the center that produce a giant vortex which is not supposed to appear in a slow rotation case.

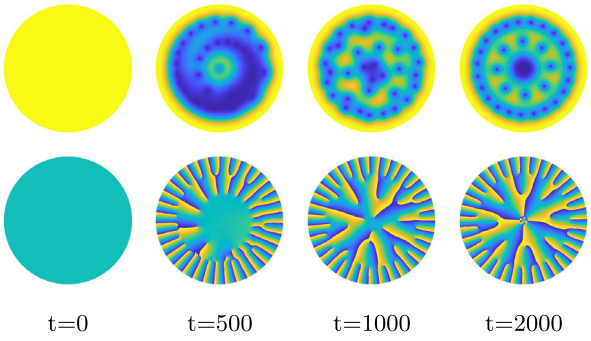

FIG. 1. Formation of a giant vortex with winding number $N = 4$ at $\Omega = 1.65$ and $R = 5$. The top row shows the order parameter, while the bottom row shows the phase configuration at the corresponding time. The temperature $T = 0.67T_c$.

When the rotational velocity exceeds 0.45, the vortices will enter the center of the hexagonal grid superfluid. The giant vortex will be discovered from Ω. Figures 2(a) and 2(b) show how two charges combine in the disk center and form a stable giant vortex. We cannot distinguish the number of charges in the disk center by order parameters alone, so we must turn to the diagram of phase configuration. In the diagram of phase configuration, the phase difference from blue to yellow is 2π, which corresponds to a single vortex. The winding number of the vortex $N = 2$, the vortex is a giant vortex. The stable giant vortex state is not a common phenomena, because multiple vortices tend to exist independently in a normal case [10]. But we discover that the giant vortex state is stable under fast rotating conditions, the situation has also been observed using the GP equation [31,32].

When $\Omega = 0.5$, the giant vortex is already shown. However, in Figs. 2(c) and 2(d), where $\Omega = 0.8$, no giant vortices appear and only four inner-layer vortices form a quartet lattice, with 11 vortices in the outer layer. This indicates the instability of the giant vortex. As the rotational velocity increases, new physical images of the holographic superfluid are constantly presented. In Figs. 2(e)–2(h), we find the vortex in the center with a two-layer lattice structure in the disk. When the dynamic system has the rotational velocity $\Omega = 1$, there is only one vortex core in the center of the disk; when $\Omega = 1.5$, there are three

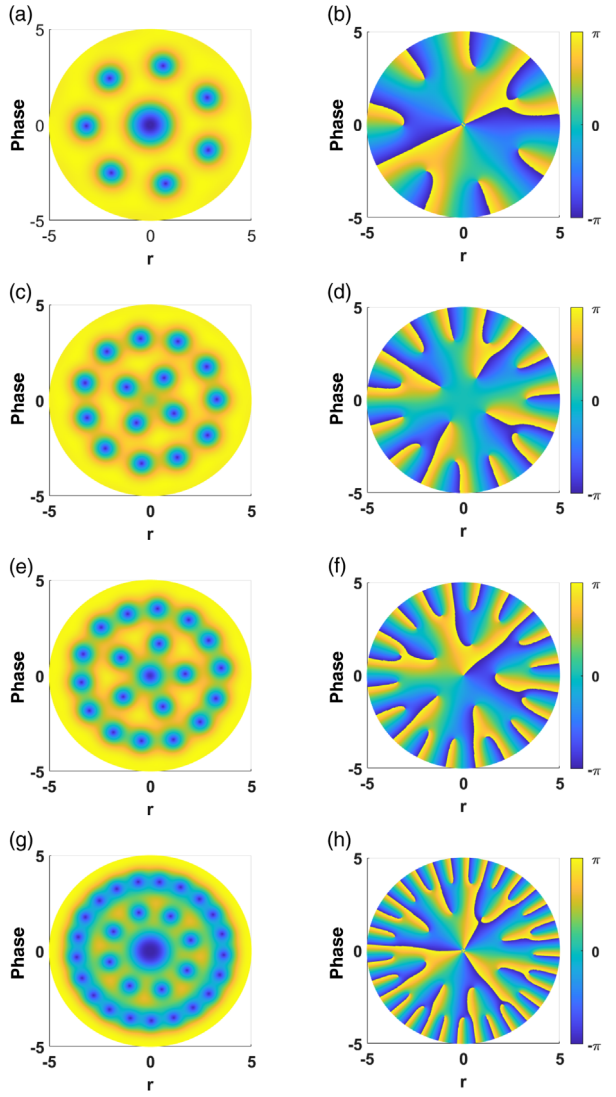

FIG. 2. Order parameter (left panels) and phase (right panels) when (a),(b) $\Omega = 0.5$, (c),(d) $\Omega = 0.8$, (e),(f) $\Omega = 1$, and (g),(h) $\Omega = 1.5$. The value of the phase varies continuously from 0 (blue) to 2π (yellow). When $\Omega = 0.5$, a giant vortex whose winding number is 2 appears at the center of the dynamic system. But when Ω is increased to 0.8, the giant vortex disappears and splits into four single charged vortices to form a square structure. In (e)–(h), the giant vortex appears and is surrounded by a two-layer vortex structure. The temperature $T = 0.67T_c$.

vortices inside the octagonal grid, and they form a state of dynamic equilibrium due to mutual interaction. We have not yet seen the emergence of a three-layer structure, which might be found in a larger disk. Figures 2(e) and 2(g) and Figs. 2(f) and 2(h) have similar structures, while in Figs. 2(g) and 2(h), the faster case, the structure of the outer layer in the left image has begun to blur. There is a clear tendency to form a ring, but the vortex of the outer layer in this picture can still be distinguished. One can count 21 vortices in the outer layer, and the inner layer is an octagonal grid. From the phase configuration on the right, it can be seen that the superfluid of the double lattice structure can also form a large winding vortex in the center when the rotational velocity is large enough. From Fig. 2, we find that the phase configuration has a hierarchical structure, and each layer corresponds to a circle of vortices in the order parameter. Through Fig. 2, we discover that the outermost phase difference is the total winding of the entire superfluid, that the second-layer phase difference includes the winding of the inner two layers, and that the phase difference of the center shows only the winding number of the giant vortex in the disk center. This can be summarized as a regular pattern: The phase difference of the nth layer (it is stipulated that the number of layers from the inside to the outside is $1, 2, 3\ldots$ in turn) always contains the phase difference of all vortexes in the nth layer.

As the rotational velocity continues to increase, we discover a new giant vortex structure which is different from the above giant vortices shown in Figs. 2(a), 2(b), 2(g), and 2(h). The difference is not observable in the order parameter diagram, but it is clearly discernible from the diagram of the phase configuration. We can see that in Fig. 3, when $\Omega = 1.7$ and 2, there is a difference only in the outer ring when we observe the order parameter, where the vortices of the outer structure form a complete ring, but we can find that the structure of the giant vortex has changed in the diagram of the phase configuration. It is confusing to confirm the number of charges if you do not know the former regular pattern. According to the just-mentioned regular pattern, it is easy to count how many charges are in a giant vortex. We mention that the phase differences of the second floor in the diagram of the phase configuration

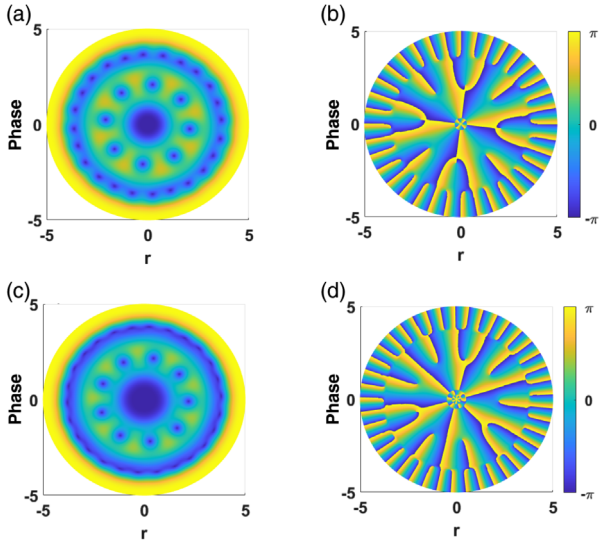

FIG. 3. Order parameter (left panels) and phase (right panels) when (a),(b) $\Omega = 1.7$ and (c),(d) $\Omega = 2$. The phase configuration of the giant vortex is stratified in both cases. We can determine a winding number of 4 in (b) and 6 in (d). The temperature $T = 0.67T_c$.

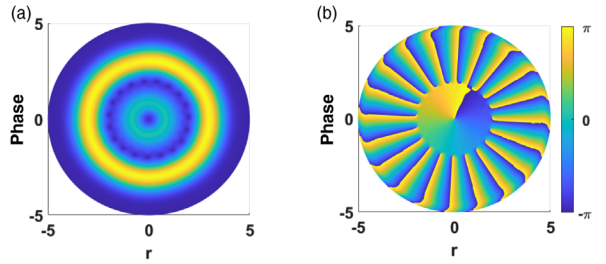

FIG. 4. (a) Order parameter and (b) phase when $\Omega = 2.5$. The order parameter in (a) shows a superfluid ring and a vortex ring. The blue ring inside is the vortex ring, while the yellow ring outside is the superfluid ring. The phase configuration is shown in (b). The temperature $T = 0.67T_c$.

(count from the outside to the inside) contains the giant vortex and is next to the giant vortex of the phase differences, so the giant vortex shown in Figs. 3(a) and. 3(b) contains a winding number $N = 4$. This means that the phase stratifies in the radius direction but that no charge emerges in the disk center. And, in the same way, we can make sure that the giant vortex on $\Omega = 2$ for Figs. 3(c) and 3(d) has a winding number $N = 6$. Notice that the phase of the giant vortex in Fig. 3(b) is divided into two layers and in Fig. 3(d) into three layers, so stratification has no relation to the number of the winding, only to Ω. In Fig. 4 with $\Omega = 2.5$, we find a superfluid ring outside and a vortex ring inside, which is similar to the result of the GP equation [57].

IV. RELATIONSHIP BETWEEN THE WINDING NUMBER AND THE ROTATING VELOCITY

We already show that as the rotating velocity increases, more vortices enter the disk and finally result in the formation of a giant vortex. Based on this fact, we give a conjecture: If Ω is large enough, a lot of vortices will emerge in the fixed size disk, a vortex can easily interact with other vortices close by due to the limited space, so several vortices can merge into a giant vortex in the disk center by overcoming the repulsive force between them. There are five regions in the overall dynamics process shown in Fig. 5. The first region of the process (in green) is a one-layer vortex lattice. The second region (in magenta) is that a giant vortex appearing in the system center based on a one-layer lattice. The situation in Figs. 2(a) and 2(b) is represented as the magenta region. The third region (in blue) is a two-layer vortex lattice. We mentioned that there is no giant vortex state in the region which corresponds to Figs. 2(c)–2(f), because the system forms a two-layer structure from a one-layer structure lattice in the rotational velocity. So vortices will not all squeeze into the middle of the disk center when the vortex quantity is not very big in the dynamics progress. The fourth region (in red) is that a giant vortex appears at the system center based on a

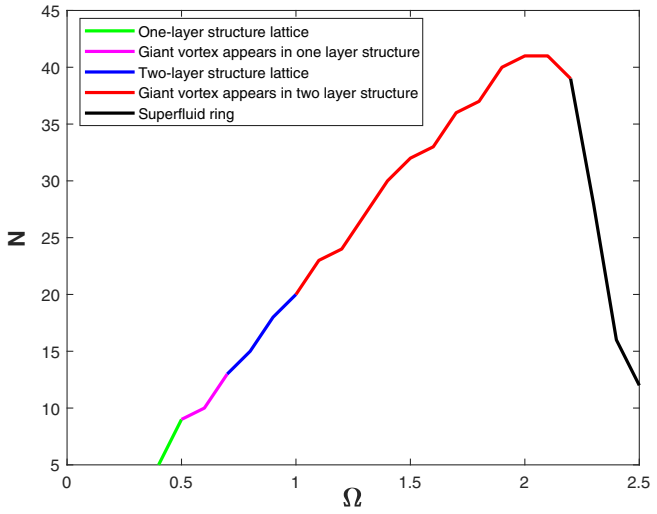

FIG. 5. Relationship between the number of vortices N and the rotating velocity Ω. The green line is the one-layer structure lattice state. The concrete physics picture of the green line is given in Ref. [53]. The magenta line represents the state of the giant vortex appearing in a one-layer structure. The blue line represents the two-layer structure lattice state in which no giant vortex arises. The red line represents the state of a giant vortex appearing in a two-layer structure. And the black line represents the superfluid ring state.

two-layer lattice. Figures 1, 2(g), 2(h), and 3 are contained in the red region. In particular, the phase of the giant vortex will stratify in this region. The fifth region (in black) is a superfluid ring and a vortex ring. The number of charges decreases rapidly with an increasing angular velocity, and the order parameter is extremely suppressed in this region. In front of the fourth region, the quantities of the vortex and the rotating velocity approximately yield the Feynman relation [54], but, obviously, as the angular velocity in the black region increases, the effect of dissipation between the vortex and the superfluid influences the Feynman relation.

V. SUMMARY

By numerically applying a holographic model on the fast rotating superfluid, we found an unusual formation of giant vortices: a giant vortex contains multiple charges and shows a phase configuration stratification in the radius direction. We also found the formation of a superfluid ring and a vortex ring in the ultrafast rotating case. Experimental developments enabled Kuga *et al.* [58] to create a confinement potential that is tighter than harmonic, thus creating a possible method to explore the nature of fast rotating BECs. Interesting, the giant vortex predicted by the holographic simulation has been observed in fast rotating BECs by using the quadratic-plus-quartic potential [59]. Moreover, the vortex ring found in a holographic simulation was also observed in the same

rapidly rotating BECs by increasing the rotation frequency. Also, in a holography with an analytical treatment, the giant vortex is found to describe an intermediate regime with large spin and charge, which connects superfluid theory with the large-spin expansion [60].

ACKNOWLEDGMENTS

This work is supported by the National Natural Science Foundation of China (Grant No. 11275233) and the Postgraduate Research and Practice Innovation Program of Jiangsu Province (Grant No. KYCX22_3450).

[1] G. B. Hess, Phys. Rev. B **15**, 5204 (1977).
[2] Y. Nago, M. Inui, R. Kado, K. Obara, H. Yano, O. Ishikawa, and T. Hata, Phys. Rev. B **82**, 224511 (2010).
[3] S. Autti, V. V. Dmitriev, J. T. Mäkinen, A. A. Soldatov, G. E. Volovik, A. N. Yudin, V. V. Zavjalov, and V. B. Eltsov, Phys. Rev. Lett. **117**, 255301 (2016).
[4] E. I. Blount and C. M. Varma, Phys. Rev. B **14**, 2888 (1976).
[5] V. M. H. Ruutu, J. Kopu, M. Krusius, Ü. Parts, B. Plaçais, E. V. Thuneberg, and W. Xu, Phys. Rev. Lett. **79**, 5058 (1997).
[6] E. Arahata and T. Nikuni, J. Low Temp. Phys. **183**, 191 (2016).
[7] T. ling Song, C. Ma, and Y. li Ma, Ann. Phys. (Amsterdam) **327**, 1933 (2012).
[8] M. Nakahara, T. Ohmi, T. Tsuneto, and T. Fujita, Prog. Theor. Phys. **62**, 874 (1979).
[9] D. L. Feder, Phys. Rev. Lett. **93**, 200406 (2004).
[10] Y. Kawaguchi and T. Ohmi, Phys. Rev. A **70**, 043610 (2004).
[11] R. E. Packard and T. M. Sanders, Phys. Rev. Lett. **22**, 823 (1969).
[12] E. J. Yarmchuk, M. J. V. Gordon, and R. E. Packard, Phys. Rev. Lett. **43**, 214 (1979).
[13] G. P. Bewley, M. S. Paoletti, K. R. Sreenivasan, and D. P. Lathrop, Proc. Natl. Acad. Sci. U.S.A. **105**, 13707 (2008).
[14] K. W. Madison, F. Chevy, W. Wohlleben, and J. Dalibard, Phys. Rev. Lett. **84**, 806 (2000).
[15] J. R. Abo-Shaeer, C. Raman, J. M. Vogels, and W. Ketterle, Science **292**, 476 (2001).
[16] P. C. Haljan, I. Coddington, P. Engels, and E. A. Cornell, Phys. Rev. Lett. **87**, 210403 (2001).
[17] E. Hodby, G. Hechenblaikner, S. A. Hopkins, O. M. Maragò, and C. J. Foot, Phys. Rev. Lett. **88**, 010405 (2001).
[18] T.-L. Ho, Phys. Today **56**, No. 6, 62 (2003).
[19] A. L. Fetter, Rev. Mod. Phys. **81**, 647 (2009).
[20] K. Kasamatsu, M. Tsubota, and M. Ueda, Phys. Rev. Lett. **91**, 150406 (2003).
[21] K. Kasamatsu and M. Tsubota, Phys. Rev. Lett. **97**, 240404 (2006).
[22] A. L. Fetter and A. A. Svidzinsky, J. Phys. Condens. Matter **13**, R135 (2001).
[23] M. Tsubota, K. Kasamatsu, and M. Ueda, Phys. Rev. A **65**, 023603 (2002).
[24] A. Aftalion, X. Blanc, and J. Dalibard, Phys. Rev. A **71**, 023611 (2005).
[25] A. L. Fetter, Phys. Rev. A **64**, 063608 (2001).
[26] D. L. Feder and C. W. Clark, Phys. Rev. Lett. **87**, 190401 (2001).
[27] U. R. Fischer and G. Baym, Phys. Rev. Lett. **90**, 140402 (2003).
[28] E. Lundh, Phys. Rev. A **65**, 043604 (2002).
[29] S. Viefers, T. H. Hansson, and S. M. Reimann, Phys. Rev. A **62**, 053604 (2000).
[30] T. Kuga, Y. Torii, N. Shiokawa, T. Hirano, Y. Shimizu, and H. Sasada, Phys. Rev. Lett. **78**, 4713 (1997).
[31] K. Kasamatsu, M. Tsubota, and M. Ueda, Phys. Rev. A **66**, 053606 (2002).
[32] T. P. Simula, A. A. Penckwitt, and R. J. Ballagh, Phys. Rev. Lett. **92**, 060401 (2004).
[33] J. Maldacena, Int. J. Theor. Phys. **38**, 1113 (1999).
[34] G. Hooft, Nucl. Phys. **B72**, 461 (1974).
[35] O. Aharony, S. S. Gubser, J. Maldacena, H. Ooguri, and Y. Oz, Phys. Rep. **323**, 183 (2000).
[36] S. S. Gubser, Phys. Rev. D **78**, 065034 (2008).
[37] S. A. Hartnoll, C. P. Herzog, and G. T. Horowitz, Phys. Rev. Lett. **101**, 031601 (2008).
[38] C. P. Herzog, P. K. Kovtun, and D. T. Son, Phys. Rev. D **79**, 066002 (2009).
[39] S. Gubser, I. Klebanov, and A. Polyakov, Phys. Lett. B **428**, 105 (1998).
[40] E. Witten, Adv. Theor. Math. Phys. **2**, 253 (1998).
[41] J. Zaanen, Y. Liu, Y.-W. Sun, and K. Schalm, *Holographic Duality in Condensed Matter Physics* (Cambridge University Press, Cambridge, England, 2015).
[42] M. Ammon and J. Erdmenger, *Gauge/Gravity Duality: Foundations and Applications* (Cambridge University Press, Cambridge, England, 2015).
[43] S. A. Hartnoll, A. Lucas, and S. Sachdev, *Holographic Quantum Matter* (MIT Press, Cambridge, MA, 2018).
[44] Y. Lahini, R. Pugatch, F. Pozzi, M. Sorel, R. Morandotti, N. Davidson, and Y. Silberberg, Phys. Rev. Lett. **103**, 013901 (2009).
[45] V. Keranen, E. Keski-Vakkuri, S. Nowling, and K. P. Yogendran, Phys. Rev. D **81**, 126012 (2010).
[46] Ó. J. C. Dias, G. T. Horowitz, N. Iqbal, and J. E. Santos, J. High Energy Phys. 04 (2014) 096.
[47] M.-S. Wu, S.-Y. Wu, and H.-Q. Zhang, J. High Energy Phys. 05 (2016) 011.
[48] K. Maeda, M. Natsuume, and T. Okamura, Phys. Rev. D **81**, 026002 (2010).
[49] O. Domènech, M. Montull, A. Pomarol, A. Salvio, and P. J. Silva, J. High Energy Phys. 08 (2010) 033.
[50] G. Tallarita, R. Auzzi, and A. Peterson, J. High Energy Phys. 03 (2019) 114.

[51] G. Tallarita and R. Auzzi, J. High Energy Phys. 01 (2020) 056.
[52] X. Li, Y. Tian, and H. Zhang, J. High Energy Phys. 02 (2020) 104.
[53] C. Y. Xia, H. B. Zeng, H. Q. Zhang, Z. Y. Nie, Y. Tian, and X. Li, Phys. Rev. D **100**, 061901(R) (2019).
[54] R. Feynman, in *Progress in Low Temperature Physics, Vol. XVI: Quantum Turbulence*, edited by M. Tsubota (Elsevier, New York, 1955), pp. 17–53.
[55] A. Adams, P. M. Chesler, and H. Liu, Science **341**, 368 (2013).
[56] See Supplemental Material at http://link.aps.org/supplemental/10.1103/PhysRevD.107.026006 for a video of the dynamical formation of a giant vortex in which $\Omega = 1.65$, $T = 0.66T_c$, and $R = 5$.
[57] N. Rougerie, Arch. Ration. Mech. Anal. **203**, 69 (2011).
[58] T. Kuga, Y. Torii, N. Shiokawa, T. Hirano, Y. Shimizu, and H. Sasada, Phys. Rev. Lett. **78**, 4713 (1997).
[59] P. Engels, I. Coddington, P. C. Haljan, V. Schweikhard, and E. A. Cornell, Phys. Rev. Lett. **90**, 170405 (2003).
[60] Gabriel Cuomo and Zohar Komargodski, arXiv:2210.15694.